









# 6 Multiomics Identifies Potential Molecular Profiles Associated With Outcomes After BRAF-Targeted Therapy in Patients With BRAF V600E-Mutated Advanced Solid Tumors

Martina Eriksen, MD, PhD<sup>1</sup> ; Anne M. Hansen, PhD<sup>2</sup>; Annelaura B. Nielsen, PhD<sup>3</sup> ; Filip Mundt, PhD<sup>3</sup> ; Matthias Mann, PhD<sup>3</sup> ; Ulrik Lassen, MD, PhD<sup>1</sup> ; Lise B. Ahlborn, PhD<sup>2</sup> ; Martin Højgaard, MD, PhD<sup>1</sup>; Iben Spanggaard, MD, PhD<sup>1</sup> ; Camilla Qvortrup, MD, PhD<sup>1</sup>; Christina W. Yde, PhD<sup>2</sup>; and Kristoffer S. Rohrberg, MD, PhD<sup>1</sup> 

DOI <https://doi.org/10.1200/PO.24.00266>

## ABSTRACT

**PURPOSE** It is a clinical challenge to select patients for BRAF-targeted therapy because of the lack of predictive biomarkers besides the BRAF V600E mutation. By analyzing the genome, transcriptome, and proteome, this study investigated the association between baseline molecular alterations and outcomes of BRAF-targeted therapy.

**PATIENTS AND METHODS** Fresh tumor tissue from patients enrolled in the Copenhagen Prospective Personalized Oncology study was collected and underwent comprehensive molecular profiling.

**RESULTS** *TP53* comutations were most frequently detected. Patients with a *TP53* wild-type tumor had a significantly longer median progression-free survival than those with *TP53* comutations (hazard ratio, 2.8 [95% CI, 1.13 to 7.08];  $P = .02$ ). RNAseq revealed a distinct gene expression signature for patients with long-term disease control (LDC), including hallmarks of cell cycle arrest and proliferation in the p53 pathway. The protein analysis demonstrated that ubiquitin-conjugating enzyme E2K was significantly downregulated in patients with LDC.

**CONCLUSION** Using a multiomic approach, we identified molecular alterations associated with treatment outcomes. The potential of analyzing multiomic data is promising and should be prioritized in translational cancer research to uncover the full potential within precision oncology.

## ACCOMPANYING CONTENT

 [Data Sharing Statement](#)

Accepted January 21, 2025

Published March 13, 2025

JCO Precis Oncol 9:e2400266

© 2025 by American Society of Clinical Oncology

Licensed under the Creative Commons Attribution 4.0 License

## INTRODUCTION

*BRAF* mutations are well known as oncogenic drivers in several cancers and are found in approximately 6% of all cases of metastatic cancer.<sup>1</sup> Activating *BRAF* mutations lead to constitutive activation of the mitogen-activated protein kinase (MAPK) pathway resulting in uncontrolled cell proliferation, dedifferentiation, and cell survival.<sup>2</sup> The most common *BRAF* mutation in human cancer is the *BRAF* V600E mutation.<sup>3,4</sup>

Although targeted therapies can be an effective strategy for treating cancer, the duration of responses to such therapies, for example, *BRAF* inhibitors (BRAFi), varies substantially and can be dependent on the origin of the primary tumor.<sup>5-11</sup>

Different molecular alterations have been proposed as predictive biomarkers of response to BRAF-targeted therapy besides the *BRAF* V600E mutation. For example, loss-of-function mutations in tumor suppressor genes have been

shown to predict a lack of sensitivity to BRAF-targeted therapy and are negatively associated with survival outcomes in melanoma.<sup>12-15</sup> By contrast, in colorectal cancer (CRC), loss-of-function mutations in specific tumor suppressor genes have been proposed to predict good response to BRAF-targeted therapy and improved survival.<sup>16,17</sup> Generally, the impact of molecular alterations regarding response and outcomes to BRAF-targeted therapy has yet to be fully elucidated.

Many proposed predictive biomarkers arise from data generated from DNA sequencing. In addition, more insights may be gained by analyzing transcriptomics and proteomics. Recently, we have enabled the extraction of material for mass spectrometry (MS)-based protein expression analyses from the same biopsy used for DNA and RNA sequencing.<sup>18</sup> Proteins are the translated product of DNA alterations and critical molecules in all biological contexts.<sup>19</sup> Additional insights, including a functional understanding of cancer signaling pathways, could potentially be gained with a multiomic approach.<sup>20-22</sup>

## CONTEXT

### Key Objective

Are there molecular alterations associated with outcomes to BRAF-targeted therapy in patients with BRAF V600E-mutated advanced solid tumors?

### Knowledge Generated

Molecular alterations associated with outcomes to BRAF-targeted therapy were found using a multiomic approach analyzing RNA and protein expression in addition to DNA sequencing. Comutational status of the tumor suppressor gene *TP53*, and expression of the protein ubiquitin-conjugating enzyme EK2 were found to be associated with outcomes to the BRAF-targeted therapy.

### Relevance

Knowledge on how molecular alterations affect outcomes to BRAF-targeted therapy in patients with BRAF V600E-mutated advanced solid tumors is an important tool that may help clinicians decide on the most appropriate therapy for the individual patient.

## Aim

This study aimed to investigate the association between baseline molecular characteristics and BRAF-targeted therapy outcomes in patients with BRAF V600E-mutated advanced solid tumors. We focused on the impact of comutations and on identifying molecular features associated with a long-term benefit of the therapy.

## PATIENTS AND METHODS

### Patient Cohort and BRAF-Targeted Therapy

This study comprises the subpopulation of patients with BRAF V600E-mutated solid tumors enrolled in the Copenhagen Prospective Personalized Oncology study (CoPPO).<sup>23</sup> CoPPO was approved by the regional ethics committee (reference No.: 1300530) and all patients signed informed consent before inclusion.

The patients in the current study were all assigned to treatment with BRAF-targeted therapy between June 2016 and January 2021 at Copenhagen University Hospital, Rigshospitalet.

All were treated with a BRAFi combined with an anti-EGFR antibody or a MEK inhibitor or both.

Clinical data were collected from electronic medical records.

### Response Evaluation

A baseline computed tomography (CT) scan was performed before the initiation of BRAF-targeted therapy, and response to treatment was evaluated with CT scans. The response was assessed according to RECIST version 1.1.<sup>24</sup>

### Long-Term Disease Control and Survival Analysis

We defined long-term disease control (LDC) as duration of the BRAF-targeted therapy lasting 1 year or more before disease progression. In the analyses concerning patients with LDC, these patients are compared with the rest of the cohort in the study.

Overall survival (OS) was calculated from the start of therapy to death of any cause. Progression-free survival (PFS) was calculated from the start of therapy until progression, according to RECIST 1.1. The Cox proportional hazards model method was used to estimate the hazard ratio (HR) and 95% CI. The survival analyses were done in R Studio, version 4.1.1.

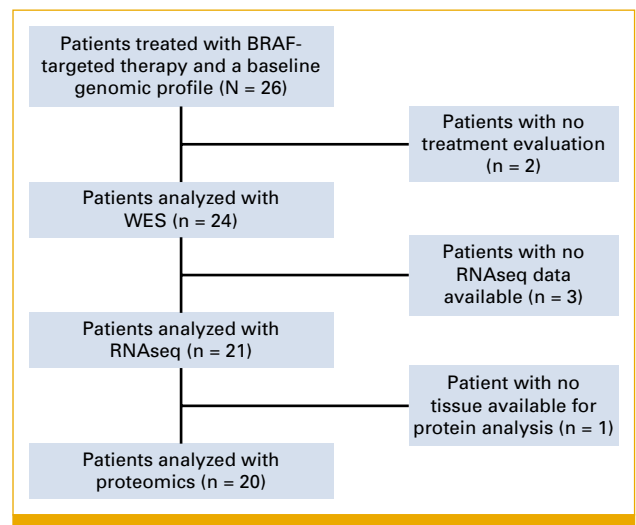


**FIG 1.** Flow diagram of the included patients. WES, whole exome sequencing.

## Biological Material

In CoPPO, fresh tumor biopsies, stored in RNAlater, from a metastatic lesion, were obtained before initiating targeted therapy. The tumor tissue was used for molecular profiling, as described below. Peripheral blood samples were also obtained to analyze germline variants and circulating tumor DNA.

## Methods for Molecular Profiling of DNA and RNA

Tumor DNA and RNA were extracted from the tissue biopsies using the AllPrep kit from QIAGEN according to the manufacturer's instructions. Germline DNA was purified from blood using a Tecan liquid handler. DNA (tumor and germline) were processed to perform whole exome sequencing by standard protocols using 10–150 ng of DNA as input. Similarly, RNA was processed for sequencing using 10–200 ng of input. Library preparation was done with SureSelect Clinical Research Exome (Agilent, Santa Clara, CA) and TruSeq Stranded Total RNA Prep Gold (Illumina, San Diego, CA). Sequencing was performed on the Illumina NovaSeq6000 system. The raw data were mapped to the hg19/GRCh37 human reference genome using BWA-MEM software, version 0.7.12. Genome Analysis Toolkit best practices were followed when calling variants.

## Mutational Analyses

DNA variants were analyzed using QIAGEN Clinical Insight Interpret. Somatic mutations were identified by subtracting the germline variants from the tumor variants. The American College of Medical Genetics and Genomics guideline<sup>25</sup> was used to interpret the cancer-associated variants. In the current study, only variants classified as pathogenic or likely pathogenic were considered.

## RNAseq Analyses

After mapping reads from the RNAseq analysis to the hg19/GRCh37 reference genome, a matrix of FeatureCounts was generated. Differentially expressed gene analysis was performed using DESeq2 (v.1.38.3) with FeatureCounts as input and based on the selected reference groups. As some patient samples contained elevated amounts of ribosomal RNA, all data sets were depleted of these genes using a gene list extracted from the RefSeq GTF database. Only genes with an adjusted *P* value of  $<.05$  were used in downstream analyses.

The Gene Set Enrichment Analysis was computed using the R-package fgsea with a preranked gene list. Gene sets were restricted to a minimum size of 15 genes and a maximum of 400. The analysis was executed on gene sets from MSigDB<sup>26</sup> using the H: hallmarks gene sets.

The heatmap was computed using the Pheatmap package on logarithm-transformed (rlog-transformed) data. Only the top 25 upregulated and downregulated genes were selected (log2FC, adjusted *P*  $<.05$ ).

The volcano plot highlights the significantly upregulated and downregulated genes (*P*  $<.05$ ).

The principal component analysis plot was generated with rlog-transformed data using the top 500 most variable genes.

## Methods for Mass Spectrometry–Based Proteomics

The complete method for the protein analyses is previously described.<sup>18</sup> Briefly, the flowthrough containing proteins remained after the extraction of DNA and RNA using the QIAGEN AllPrep kit. In summary, ice-cold (–20°C) acetone

**TABLE 1.** Demographics and Clinical Characteristics of Patients (N = 24)

| Characteristic                          | Number of Patients |
|---|--------------------|
| Sex                                     |                    |
| Male                                    | 14                 |
| Female                                  | 10                 |
| Age, years                              |                    |
| Median                                  | 62                 |
| Range                                   | 33-80              |
| Primary tumors                          |                    |
| Colon cancer                            | 15                 |
| NSCLC                                   | 3                  |
| NEC                                     | 2                  |
| MiNEN                                   | 1                  |
| Cholangiocarcinoma                      | 1                  |
| Breast cancer                           | 1                  |
| MM                                      | 1                  |
| BRAF-targeted therapy regimen           |                    |
| Dabrafenib + trametinib                 | 5                  |
| Dabrafenib + trametinib + panitumumab   | 4                  |
| Vemurafenib + panitumumab               | 4                  |
| Vemurafenib + panitumumab + irinotecan  | 3                  |
| Vemurafenib + cobimetinib               | 1                  |
| Encorafenib + binimetinib + panitumumab | 3                  |
| Encorafenib + panitumumab               | 2                  |
| Encorafenib + binimetinib               | 1                  |
| Treatment duration, weeks               |                    |
| Median                                  | 32                 |
| Range                                   | 8-230              |
| Best radiologic response                |                    |
| CR                                      | 1                  |
| PR                                      | 16                 |
| SD                                      | 7                  |
| PD                                      | 0                  |

NOTE. Sex, median age, primary tumors, BRAF-targeted therapy regimens, duration of therapy (in rounded weeks) until progression, and the best radiologic response according to RECIST 1.1 are summarized. Abbreviations: CR, complete response; MiNEN, mixed neuroendocrine non-neuroendocrine neoplasm; MM, malignant melanoma; NEC, neuroendocrine carcinoma; NSCLC, non-small cell lung cancer; PD, progressive disease; PR, partial response; SD, stable disease.

(100%) was added to each sample in a total of four volumes. The mixture was inverted a few times and kept overnight at  $-20^{\circ}\text{C}$ . The following day, a clearly visible cloudy precipitate had formed. After centrifugation for 10 minutes at 20,000 relative centrifugal force (RCF) at  $4^{\circ}\text{C}$ , the supernatant was removed, and the pellet was washed with approximately 500  $\mu\text{L}$  of ice-cold ( $-20^{\circ}\text{C}$ ) acetone. The pellet was then air-dried for approximately 10 minutes, or until no liquid remained above it, without being overdried. Pellets were resuspended in 8M urea using sonication (Bioruptor Plus, with 15 cycles of 30 seconds on and 30 seconds off). For digestion, we added LysC at a 1:50 ratio (enzyme:protein; w/w) and incubated for 2 hours on a shaker at 800 rpm. The 8M urea was diluted four times down to 2M urea in 50 mM Tris-HCl (pH 8.0) buffer. Then we added trypsin at the same ratio and incubated overnight on a shaker at 800 rpm. The next day, digestion was stopped by acidification using formic acid (FA) to a final concentration of 1%.

To desalt, Sep-Pak cartridges tC18 (3 cc 200 mg) were used. Cartridges were initially conditioned with 2 mL of 100% acetonitrile (ACN), followed by 2 mL of 50% ACN/0.1% FA. Next, they were equilibrated with  $4 \times 2$  mL of 0.1% TFA. The

samples were centrifuged at 20,000 RCF for 10 minutes before loading onto the cartridge. The cartridge was washed/desalted with  $3 \times 2$  mL of 0.1% trifluoroacetic acid (TFA), followed by washing/desalting with 2 mL of 1% FA to remove the TFA. The elution was performed using  $2 \times 1$  mL of 50% ACN/0.1% FA. The eluate was then dried by speed-vacuuming at  $45^{\circ}\text{C}$  and resuspended in 50  $\mu\text{L}$  of A\*. Finally, the sample was ready for peptide concentration determination using the NanoDrop spectrophotometer (Thermo Scientific, Waltham, MA).

### Liquid Chromatography and Tandem Mass Spectrometry Analyses

Two-hundred ng of digested peptides were loaded onto a disposable Evotip C18 trap column (Evosep Biosystems, Odense, Denmark). The Evotips were primed with 2-propanol and activated with 0.1% FA in ACN, followed by equilibration with 0.1% FA. Centrifugal force at 800 RCF for 1 minute was used to load the Evotips onto the trap column. Once loaded, the Evotips were washed with 0.1% FA, and 200  $\mu\text{L}$  of 0.1% FA was added to the top of the disks to prevent drying. The Evosep One LC system (Evosep Biosystems) was

| Patient ID       | 4   | 9   | 5   | 18 | 16  | 7   | 23  | 19 | 13 | 8  | 17  | 11 | 20  | 21  | 3   | 15  | 12  | 2   | 6   | 10  | 14  | 24  | 1   | 22 |
|------------------|-----|-----|-----|----|-----|-----|-----|----|----|----|-----|----|-----|-----|-----|-----|-----|-----|-----|-----|-----|-----|-----|----|
| Cancer           | LC  | Col | Col | BC | NEC | NEC | Col | CC | MN | MM | Col | LC | Col | Col | Col | Col | Col | Col | Col | Col | Col | Col | Col | LC |
| Therapy Duration | 230 | 116 | 95  | 65 | 56  | 47  | 38  | 38 | 36 | 36 | 35  | 33 | 31  | 30  | 27  | 26  | 24  | 18  | 16  | 15  | 15  | 12  | 10  | 8  |
| TP53             |     |     |     |    |     |     |     |    |    |    |     |    |     |     |     |     |     |     |     |     |     |     |     |    |
| APC              |     |     |     |    |     |     |     |    |    |    |     |    |     |     |     |     |     |     |     |     |     |     |     |    |
| PIK3CA           |     |     |     |    |     |     |     |    |    |    |     |    |     |     |     |     |     |     |     |     |     |     |     |    |
| MTOR             |     |     |     |    |     |     |     |    |    |    |     |    |     |     |     |     |     |     |     |     |     |     |     |    |
| PTEN             |     |     |     |    |     |     |     |    |    |    |     |    |     |     |     |     |     |     |     |     |     |     |     |    |
| NF1              |     |     |     |    |     |     |     |    |    |    |     |    |     |     |     |     |     |     |     |     |     |     |     |    |
| AKT1             |     |     |     |    |     |     |     |    |    |    |     |    |     |     |     |     |     |     |     |     |     |     |     |    |
| ARID1A           |     |     |     |    |     |     |     |    |    |    |     |    |     |     |     |     |     |     |     |     |     |     |     |    |
| JAK2             |     |     |     |    |     |     |     |    |    |    |     |    |     |     |     |     |     |     |     |     |     |     |     |    |
| RNF43            |     |     |     |    |     |     |     |    |    |    |     |    |     |     |     |     |     |     |     |     |     |     |     |    |
| IDH1             |     |     |     |    |     |     |     |    |    |    |     |    |     |     |     |     |     |     |     |     |     |     |     |    |
| CDKN2A           |     |     |     |    |     |     |     |    |    |    |     |    |     |     |     |     |     |     |     |     |     |     |     |    |
| ERBB3            |     |     |     |    |     |     |     |    |    |    |     |    |     |     |     |     |     |     |     |     |     |     |     |    |
| KDM6A            |     |     |     |    |     |     |     |    |    |    |     |    |     |     |     |     |     |     |     |     |     |     |     |    |
| MSH6             |     |     |     |    |     |     |     |    |    |    |     |    |     |     |     |     |     |     |     |     |     |     |     |    |
| MSH3             |     |     |     |    |     |     |     |    |    |    |     |    |     |     |     |     |     |     |     |     |     |     |     |    |
| BRCA1            |     |     |     |    |     |     |     |    |    |    |     |    |     |     |     |     |     |     |     |     |     |     |     |    |
| BRCA2            |     |     |     |    |     |     |     |    |    |    |     |    |     |     |     |     |     |     |     |     |     |     |     |    |

**FIG 2.** Baseline comutations in patients with BRAF V600E mutated solid tumors. Primary cancer, duration of response, and comutational status per patient are illustrated. The numbers at the top represent each patient, and primary cancer and therapy duration in weeks (rounded to the nearest whole week) is below. The bright green background in therapy duration marks patients with long-term disease control (more than 1 year). The colored boxes show that the patient had a mutation in the specific gene mentioned: red boxes represent gain-of-function mutations, and blue boxes loss-of-function mutations. \*In this patient, a *PTEN* gene fusion was detected. BC, breast cancer; CC, cholangiocarcinoma; Col, colon cancer; ID, identification; LC, lung cancer (all non-small cell lung cancer); MM, malignant melanoma; MN, mixed neuroendocrine non-neuroendocrine neoplasm; NEC, neuroendocrine carcinoma.

used to transfer the mass spec–ready peptides to a mass spectrometer. The peptides were eluted and separated by a 15-cm PepSep column (150  $\mu$ m inner diameter; Evosep) filled with 1.5  $\mu$ m Reprosil–Pur C18 beads (Dr Maisch GmbH, Germany) using a standardized Evosep 44-minute gradient method. Buffer A (0.1% FA in MS–grade water) and buffer B (0.1% FA in ACN) were used during the process, and the column temperature was maintained at 60°C using a Sonation Nanospray Flex Column oven. The total sample throughput was 30 samples per day (30 SPDs).

The Trapped Ion Mobility Spectrometry (TIMS) quadrupole time-of-flight (TOF) mass spectrometer (Bruker timsTOF Pro or timsTOF SCP) was used in data-independent acquisition mode with TIMS. The liquid chromatographer was coupled to the hybrid TIMS quadrupole TOF mass spectrometer through a 15-cm Pepsep column. For data-independent acquisition parallel accumulation-serial fragmentation (diaPASEF), the method covered an  $m/z$ -range of 100–1,700 at MS1 to 400–1,200 at MS2. The method included two ion mobility windows per diaPASEF scan, with variable isolation window widths adjusted to precursor densities. Twenty-five diaPASEF scans were deployed at a throughput of 30 SPDs with a cycle time of 2.7 seconds. The ion mobility range was set to 1.6 Vs  $\text{cm}^{-2}$  and 0.6 Vs  $\text{cm}^{-2}$ , and accumulation and ramp times were specified as 100 ms for all experiments. The collision energy was set from 20 eV (0.6 Vs  $\text{cm}^{-2}$ ) to 59 eV at 1/K0 (1.6 Vs  $\text{cm}^{-2}$ ).

DIA-NN 1.8.0.1 was used to search the proteomes, with a maximum mass accuracy tolerance of 15 ppm for MS1 and MS2 spectra. Trypsin/P was set as the protease, with up to one missed cleavage and a maximum of two variable modifications from a list of modifications. Precursor lengths ranged from 7 to 30 amino acids with a charge of 2 or 3. MBR was used for proteome analysis, and protein inference was turned off. Spectral library was generated on-the-fly, and proteotypic peptides were annotated using the “Reannotate” option in DIA-NN. Quantification mode was set to “Robust LC (high precision),” and the output was filtered on the basis of precursor  $q$ -value <1% and global protein  $q$ -value <1%.

### Protein Analyses

DIAnn data output was processed using the Clinical Knowledge Graph.<sup>27</sup> After removing proteins with a high number of missing values (maximum 30% missing values), missing values were imputed on the basis of a normal distribution (width = 0.3; downshift = 1.8). For the pairwise comparison of the low-response group to the LDC group, a two-sided unpaired  $t$ -test was performed. We applied a Benjamini–Hochberg false discovery rate of 5% to correct for multiple hypothesis testing. Proteins below this threshold are referred to as significant, whereas proteins with a  $P < .05$  before multiple hypothesis correction are, in this study, referred to as protein candidates.

Pearson correlations between RNA and protein measurements were computed from a subset of the data where RNA

and protein were measured for the same genes ( $n = 6,830$ ) and samples ( $n = 20$ ). RNA measures were the norm-transformed output from DESeq2, and protein measures were  $\log_2(\text{label-free quantification [LFQ]})$  from DIAnn.

Volcano plot: red dots highlight the proteins with a  $P < .05$  and a positive  $\log_2\text{FC}$ , while light blue dots represent the proteins with a  $P < .05$  and a negative  $\log_2\text{FC}$ . The dark blue protein highlights the protein with a post hoc adjusted  $P < .05$ .

The heatmap was computed using the cluster-map package in python seaborn, selecting the top 25 upregulated and downregulated proteins on the basis of the  $\log_2\text{FC}$  among proteins with a  $P < .05$  before correction in long-term versus short-term disease control. Patients were clustered on the basis of the protein profile ( $z$ -scored LFQ intensities).

The protein-protein correlation was computed on the basis of a data set of all proteins with a  $P < .05$  before correction.

## RESULTS

### Included Patients

Patients with a BRAF V600E-mutated, advanced solid tumor treated with BRAF-targeted therapy were identified. Figure 1 shows the flow diagram of the included patients.

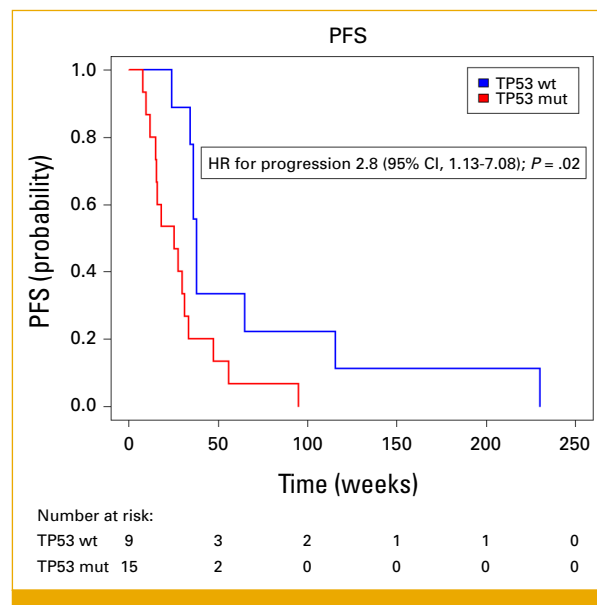


**FIG 3.** Kaplan-Meier plot of PFS in weeks in patients with BRAF V600E-mut solid tumors treated with BRAF-targeted therapy. The blue curve represents the subgroup of patients with no concurrent mutation in *TP53* at baseline. The red curve represents the patients with one or more *TP53* mutation(s) at baseline. There is a statistically significant difference in median PFS of 12.4 weeks between the two subgroups of patients (HR, 2.8 [95% CI, 1.13 to 7.08];  $P = .02$ ). HR, hazard ratio; mut, mutated; PFS, progression-free survival; wt, wild-type.



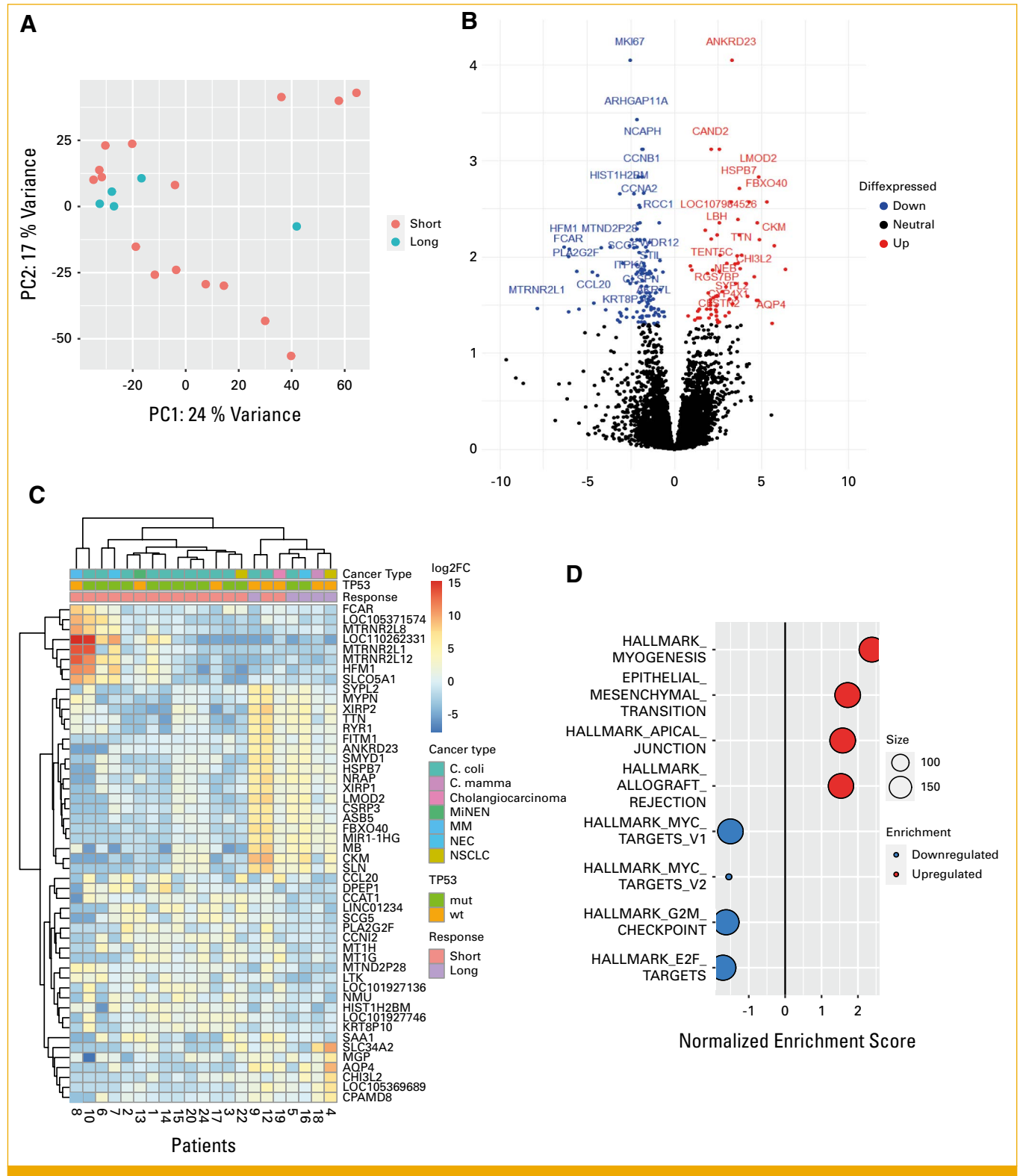


**FIG 4.** Gene expression profile in patients with LDC on the basis of RNAseq. (A) A PCA plot of patients with LDC (over 1 year) versus patients with shorter disease control (comprising rlog-transformed data using the top 500 most variable genes) showing that four of five patients clustered together. (B) A volcano plot of the significant ( $P < .05$ ) differentially expressed genes in patients with LDC versus patients with shorter disease control. Seventy genes were significantly upregulated (red dots), and 124 genes were significantly downregulated (blue dots),  $P < .05$ , in patients with LDC. (C) A heatmap of the top 25 upregulated and downregulated genes (adjusted  $P < .05$ ) with logarithmically transformed data. Patients were clustered on the basis of the deregulated genes, and a gene expression signature was indicated. Primary cancer, TP53 mutational status, and duration of disease control are depicted at the top. (D) A GSEA plot illustrating upregulated and downregulated cancer hallmarks in patients with LDC versus shorter disease control. Pathways involved in cell cycle and (continued on following page)

**FIG 4.** (Continued). proliferation were downregulated in patients with LDC. FC, fold change; GSEA, Gene Set Enrichment Analysis; LDC, long-term disease control; MiNEN, mixed neuroendocrine non-neuroendocrine neoplasm; MM, malignant melanoma; mut, mutated; NEC, neuroendocrine carcinoma; NSCLC, non-small cell lung cancer; PC, principal component; PCA, principal component analysis; wt, wild-type.

**Table 1** summarizes the demographics and clinical characteristics of the 24 included patients. Seven different histologies were represented. The BRAF-targeted therapy continued until progressive disease, and the best radiologic responses are reported in **Table 1**.

## Results of Mutational Analyses

BRAF V600E mutation was detected in all included patients. Variants in the tumor suppressor gene *TP53*, resulting in loss of function, were the most frequently detected comutation (**Fig 2**). 62.5% (15/24) of the patients had at least one *TP53* comutation, with one patient having two comutations in *TP53*. For other variants found, consult **Figure 2**.

### Impact of Comutations on Survival

Patients with *TP53* wild-type (wt) tumors had a statistically significant longer median PFS of 12.4 weeks compared with patients with *TP53* comutated tumors (HR, 2.8 [95% CI, 1.13 to 7.08];  $P = .02$ ; **Fig 3**). The median OS was 78.6 weeks in the *TP53* wt subgroup of patients and 57.1 weeks in the *TP53*-mutated subgroup, but this difference was not statistically significant (HR, 1.3 [95% CI, 0.54 to 3.2];  $P = .6$ ). None of the other comutations were associated with survival.

## Results of RNAseq

RNAseq data showed a distinct expression signature in patients with LDC (**Fig 4**). However, two patients with shorter disease control seemed to cluster with those with LDC (**Fig 4C**): one patient had colon cancer and disease control for 24 weeks until progression, and one had cholangiocarcinoma and disease control for 38 weeks. We observed a downregulation of cell cycle and proliferation hallmarks in the p53 pathway (**Fig 4D**).

## Results From Protein Analyses

On the basis of the expression profile from the RNAseq data in patients with LDC, we wanted to explore the protein expression in this subgroup.

Approximately 300 proteins were found to be differentially expressed ( $P < .05$ ) among patients with LDC and the rest of the cohort (data not shown). After multiple hypothesis corrections, only one protein was significantly differentially expressed in the two groups: ubiquitin-conjugating enzyme E2K (UBE2K),<sup>28</sup> which was significantly downregulated in patients with LDC (**Fig 5A**). In two patients, we had paired samples available for the protein analyses. In those two

patients, we could detect that the abundance of UBE2K increased at the time of progression (**Fig 5B**).

The protein-protein correlation indicated similarities in protein expression in patients with LDC and revealed that patients cluster according to the duration of treatment, with a high, medium, and low cluster (**Fig 5C**). When clustering the patients on the basis of the top 25 upregulated and downregulated protein candidates, we identified protein expression profiles associated with LDC (**Fig 5D**).

Overall, the correlation between RNA and protein was low, around 0.4 (**Fig 5E**).

## DISCUSSION

In our study, using a multiomic approach, we identified potential predictive biomarkers of response to BRAF-targeted therapy in patients with BRAF V600E-mutated advanced solid tumors.

*TP53* is a tumor suppressor gene and is involved in the regulation of cell growth.<sup>29</sup> *TP53* is essential for maintaining genomic stability and preventing oncogenic transformation,<sup>30</sup> and is the most frequently mutated gene in human cancer. In our study, patients with tumors that were *TP53* wt had a significantly longer median PFS than patients with *TP53* comutations (HR, 2.8 [95% CI, 1.13 to 7.08];  $P = .02$ ); however, this did not translate into a statistically significant difference in survival. These findings align with an exploratory study in BRAF V600E-mutated melanoma.<sup>14</sup>

Other tumor suppressor genes have been associated with outcomes of BRAF-targeted therapy. For example, a cell-line study identified loss-of-function mutations in *NF1* (a negative regulator of RAS activity) in tumors that were intrinsically resistant to treatment with BRAFi.<sup>12</sup> In our study, one patient with colon cancer had a comutation in *NF1*: this patient had disease control on BRAF-targeted therapy for 16 weeks before progression. Another biomarker recently proposed as predictive for response to BRAF-targeted therapy in BRAF V600E-mutated CRC is loss-of-function mutations in *RNF43*.<sup>17</sup> Elez et al<sup>17</sup> included 46 patients with metastatic CRC and found that 43% harbored a comutation in *RNF43*. In patients with microsatellite stable (MSS) disease, comutations in *RNF43* were associated with improved efficacy outcomes after BRAF-targeted therapy compared with patients with wt *RNF43* tumors.<sup>17</sup> In our study, 13 patients had MSS colon cancer. We detected only one *RNF43* mutation (c.770dupG, p.E258\*—a predicted loss-of-function mutation). This patient was treated with encorafenib and





**FIG 5.** (Continued). was calculated and clustered according to correlation profiles. (D) A heatmap of the top 25 upregulated and downregulated protein candidates with a  $P < .05$  before correction in long-term versus short-term disease control. Patients were clustered on the basis of the expression of proteins (zscored LFQ intensities). Primary cancer type, *TP53* mutational status (red box = mutated, blue box = wild-type), LDC (red box = yes, blue box = no), and duration of therapy (the darker the color, the longer the duration) are depicted at the top. (E) A correlation matrix between the measured RNA and protein samples. The correlation is calculated using the Pearson correlation. The turquoise boxes on the top represent the RNA samples, and the light orange boxes represent the protein samples. The color palette illustrates each patient in the second line from the top. The overall correlation is shown to be approximately 0.4. Twenty of the 21 patients from the RNAseq analyses were included in the protein analyses (Fig 1). The one patient with no tissue available for the protein analyses had LDC; therefore, four of the five patients with LDC were included in the protein analyses. FC, fold change; ID, identification; LDC, long-term disease control; LFQ, label-free quantification; MINEN, mixed neuroendocrine non-neuroendocrine neoplasm; MM, malignant melanoma; NEC, neuroendocrine carcinoma; NSCLC, non-small cell lung cancer; UBE2K, ubiquitin-conjugating enzyme E2.

panitumumab, and achieved partial response as the best response. However, the duration of response was only 12 weeks in this patient. Another finding in the study by Elez et al<sup>17</sup> is the suggestion of a cross-talk between the MAPK pathway and the WNT pathway that may play a role regarding the antitumor activity of BRAF-targeted therapy in patients with CRC. Another tumor suppressor gene involved in the WNT pathway is APC. APC is the most frequently mutated oncogenic driver in CRC.<sup>31</sup> In a study analyzing tumors from 468 molecular unselected patients with CRC, APC was found to have a prognostic value in predicting survival.<sup>32</sup> Of interest, tumors lacking any APC mutations were found to have an inferior prognosis than tumors harboring only one APC mutation. However, two APC mutations, alongside mutations in KRAS and TP53, exhibited the poorest prognosis of all.<sup>32</sup> In our study, six patients had at least one APC mutation. We did not observe an impact of APC mutational status on survival. However, one patient had two APC mutations concurrent with a TP53 mutation and this patient had an OS of 17 weeks. This is a very limited OS, one of the shortest in our overall cohort. As expected, we did not detect any mutations in KRAS in our study, as KRAS and BRAF V600E mutations are considered mutually exclusive.<sup>33</sup>

Achieving LDC is a clinically meaningful goal in the advanced cancer setting. In our study, we found a distinct gene expression signature and a downregulation of cell cycle and proliferation hallmarks in the p53 pathway in patients with LDC. Of the five patients with LDC, three patients had TP53 wt tumors, and two patients had a TP53 mutation. Therefore, we speculate whether this implies functional differences in p53 regardless of the mutational status of TP53.

We found one protein, UBE2K, to be significantly downregulated in patients with LDC. To our knowledge, UBE2K has not previously been associated with outcomes in BRAF-mutated cancer. UBE2K is a part of the family of enzymes involved in linking glycine residues of ubiquitin to specific lysine residues of target proteins. It is highly expressed in the brain and associated with the neurologic disorder Huntington's disease.<sup>34,35</sup> In cancer, it has been found that the expression of UBE2K is increased in hepatocellular carcinoma

(HCC), and recently it was shown that UBE2K promotes progression of HCC.<sup>36</sup> UBE2K seems to play an essential role in the regulation of cancer cell cycles and may be a target for anticancer therapy.<sup>36-39</sup> The potential role of UBE2K in BRAF V600E-mutated cancer needs further investigation.

The major limitation of the current study is the small sample size. Furthermore, the study did not include any control data. We included patients with different primary tumors in our study, which may contribute to heterogeneity of the population. However, we found UBE2K significantly downregulated in patients with LDC across four different BRAF-mutated primary tumors. Furthermore, the patients in our study represent a highly selected group of patients and may constitute another population than patients treated with BRAF-targeted therapy in daily routine practice.

In conclusion, in the surge of reaching the goal of precision oncology, it is key to be able to identify patients who will benefit the most from a specific therapy, as it seems to delay the development of acquired resistance, generally hindering a durable clinical benefit.<sup>40-43</sup>

We found that TP53 mutational status was related to PFS. By RNAseq, we demonstrated that patients with LDC had downregulation in cell cycle and proliferation hallmarks in the p53 pathway. Proteomic data revealed that one protein, UBE2K, was significantly downregulated in patients with LDC across four different histologies. Although the expression of UBE2K is known to have a prognostic value in HCC, any potential role of UBE2K in BRAF-mutated cancer has not been established. The limited sample size in our study must be carefully considered, and therefore, any conclusions regarding UBE2K in BRAF-mutated cancer cannot be made.

The findings of our study need further validation, preferably in larger prospective patient cohorts. The potential implications of analyzing transcriptomics and proteomics, in addition to genomics, seem to provide valuable new insights and should be a prioritized focus for translational cancer research in the future.

## AFFILIATIONS

<sup>1</sup>Department of Oncology, Rigshospitalet, Copenhagen University Hospital, Copenhagen, Denmark

<sup>2</sup>Department of Genomic Medicine, Rigshospitalet, Copenhagen University Hospital, Copenhagen, Denmark

<sup>3</sup>Novo Nordisk Foundation Center for Protein Research, University of Copenhagen, Copenhagen, Denmark

## CORRESPONDING AUTHOR

Martina Eriksen, MD, PhD; e-mail: [martina.amnitzboell.eriksen@regionh.dk](mailto:martina.amnitzboell.eriksen@regionh.dk).

## PRIOR PRESENTATION

Presented in part as a poster presentation at the EORTC-NCI-AACR (ENA) symposium, Barcelona, Spain, October 26-28, 2022.

## SUPPORT

Supported by a grant from the Danish patient organization the Danish Cancer Society.

## DATA SHARING STATEMENT

A data sharing statement provided by the authors is available with this article at DOI <https://doi.org/10.1200/PO.24.00266>. The data underlying this manuscript are sensitive in nature as they include human subject data, and therefore, the data cannot be made publicly available.

## AUTHOR CONTRIBUTIONS

**Conception and design:** Martina Eriksen, Annelaura B. Nielsen, Filip Mundt, Matthias Mann, Ulrik Lassen, Camilla Qvortrup, Kristoffer S. Rohrberg

**Administrative support:** Ulrik Lassen, Kristoffer S. Rohrberg

**Provision of study materials or patients:** Iben Spanggaard, Kristoffer S. Rohrberg

**Collection and assembly of data:** Martina Eriksen, Annelaura B. Nielsen, Filip Mundt, Iben Spanggaard, Camilla Qvortrup, Kristoffer S. Rohrberg

**Data analysis and interpretation:** All authors

**Manuscript writing:** All authors

**Final approval of manuscript:** All authors

**Accountable for all aspects of the work:** All authors

## AUTHORS' DISCLOSURES OF POTENTIAL CONFLICTS OF INTEREST

The following represents disclosure information provided by authors of this manuscript. All relationships are considered compensated unless otherwise noted. Relationships are self-held unless noted. I = Immediate Family Member, Inst = My Institution. Relationships may not relate to the subject matter of this manuscript. For more information about ASCO's conflict of interest policy, please refer to [www.asco.org/rwc](http://www.asco.org/rwc) or [ascopubs.org/po/author-center](http://ascopubs.org/po/author-center).

Open Payments is a public database containing information reported by companies about payments made to US-licensed physicians ([Open Payments](http://OpenPayments.org)).

## REFERENCES

1. Zehir A, Benayed R, Shah RH, et al: Mutational landscape of metastatic cancer revealed from prospective clinical sequencing of 10,000 patients. *Nat Med* 23:703-713, 2017
2. Yaeger R, Corcoran RB: Targeting alterations in the RAF-MEK pathway. *Cancer Discov* 9:329-341, 2019
3. Fedorenko IV, Paraiso KHT, Smalley KSM: Acquired and intrinsic BRAF inhibitor resistance in BRAF V600E mutant melanoma. *Biochem Pharmacol* 82:201-209, 2011

### Martina Eriksen

**Consulting or Advisory Role:** Pierre Fabre

**Travel, Accommodations, Expenses:** Pierre Fabre

### Filip Mundt

**Employment:** Novo Nordisk

**Stock and Other Ownership Interests:** Novo Nordisk

### Matthias Mann

**Stock and Other Ownership Interests:** Evosep

### Ulrik Lassen

**Honoraria:** Bayer, Pfizer, Novartis

**Consulting or Advisory Role:** Bayer, Pfizer

**Research Funding:** BMS (Inst), Roche (Inst), Pfizer (Inst), GlaxoSmithKline (Inst), Incyte (Inst), Lilly (Inst)

### Martin Højgaard

**Stock and Other Ownership Interests:** Bavarian Nordic

**Travel, Accommodations, Expenses:** Repare Therapeutics

**Uncompensated Relationships:** Repare Therapeutics, Amgen (Inst), Servier (Inst), Kinnate Biopharma (Inst), Eikon Therapeutics (Inst), Incyte (Inst)

### Iben Spanggaard

**Honoraria:** AstraZeneca

**Research Funding:** Roche (Inst), Puma Biotechnology (Inst), Pfizer (Inst), MSD (Inst), Genmab (Inst), Genentech (Inst), Bristol Myers Squibb (Inst), Orion (Inst), Loxo/Bayer (Inst), Loxo/Lilly (Inst), Symphogen (Inst), Incyte (Inst), Novartis (Inst), AstraZeneca (Inst), Amgen (Inst), Boehringer Ingelheim (Inst), Bayer (Inst), Repare Therapeutics (Inst), BioNTech SE (Inst), CDR-Life (Inst), Bioinvent (Inst), MonTa Biosciences (Inst), Dragonfly Therapeutics (Inst)

**Travel, Accommodations, Expenses:** AstraZeneca, Incyte

### Camilla Qvortrup

**Consulting or Advisory Role:** Merck KGaA, Pierre Fabre

**Research Funding:** Roche (Inst), MSD Oncology (Inst), Servier (Inst), Pfizer (Inst), Miratis (Inst), Pierre Fabre (Inst)

**Travel, Accommodations, Expenses:** Roche (Inst), Servier (Inst), Merck KGaA (Inst), Pierre Fabre (Inst)

### Kristoffer S. Rohrberg

**Honoraria:** MSD

**Consulting or Advisory Role:** Genmab, AbbVie

**Research Funding:** Lilly (Inst), Roche/Genentech (Inst), Bristol Myers Squibb (Inst), Symphogen (Inst), Pfizer (Inst), Novartis (Inst), Loxo (Inst), Bayer (Inst), Alligator Bioscience (Inst), Incyte (Inst), Genmab (Inst), Puma Biotechnology (Inst), Orion Clinical (Inst), MonTa Biosciences (Inst), Bioinvent (Inst), AstraZeneca (Inst), Merus (Inst), Repare Therapeutics (Inst), Turning Point Therapeutics (Inst), Navire (Inst), MSD (Inst), GlaxoSmithKline (Inst), BioNTech SE (Inst)

**Travel, Accommodations, Expenses:** AstraZeneca (Inst)

No other potential conflicts of interest were reported.

## ACKNOWLEDGMENT

The authors thank the patients included in the CoPPO study and their relatives.

4. Davies H, Bignell GR, Cox C, et al: Mutations of the BRAF gene in human cancer. *Nature* 417:949-954, 2002
5. Di Nicolantonio F, Vitiello PP, Marsoni S, et al: Precision oncology in metastatic colorectal cancer—From biology to medicine. *Nat Rev Clin Oncol* 18:506-525, 2021
6. Hyman DM, Puzanov I, Subbiah V, et al: Vemurafenib in multiple nonmelanoma cancers with BRAF V600 mutations. *N Engl J Med* 373:726-736, 2015
7. Flaherty KT, Puzanov I, Kim KB, et al: Inhibition of mutated, activated BRAF in metastatic melanoma. *N Engl J Med* 363:809-819, 2010
8. Sosman JA, Kim KB, Schuchter L, et al: Survival in BRAF V600-mutant advanced melanoma treated with vemurafenib. *N Engl J Med* 366:707-714, 2012
9. Kopetz S, Desai J, Chan E, et al: PLX4032 in metastatic colorectal cancer patients with mutant BRAF tumors. *J Clin Oncol* 28, 2010 (suppl 15; abstr 3534)
10. Kopetz S, Desai J, Chan E, et al: Phase II pilot study of vemurafenib in patients with metastatic BRAF-mutated colorectal cancer. *J Clin Oncol* 33:4032-4038, 2015
11. Bivona TG, Doebele RC: A framework for understanding and targeting residual disease in oncogene-driven solid cancers. *Nat Med* 22:472-478, 2016
12. Whittaker SR, Theurillat JP, Van Allen E, et al: A genome-scale RNA interference screen implicates NF1 loss in resistance to RAF inhibition. *Cancer Discov* 3:350-362, 2013
13. Tarhini A, Kudchadkar RR: Predictive and on-treatment monitoring biomarkers in advanced melanoma: Moving toward personalized medicine. *Cancer Treat Rev* 71:8-18, 2018
14. Yan Y, Robert C, Larkin J, et al: Genomic features of complete responders (CR) versus fast progressors (PD) in patients with BRAFV600-mutated metastatic melanoma treated with cobimetinib + vemurafenib or vemurafenib alone. *Ann Oncol* 27:v379, 2016
15. Nathanson KL, Martin AM, Wubbenhorst B, et al: Tumor genetic analyses of patients with metastatic melanoma treated with the BRAF inhibitor dabrafenib (GSK2118436). *Clin Cancer Res* 19:4868-4878, 2013
16. Huijberts SCFA, Boelens MC, Bernards R, et al: Mutational profiles associated with resistance in patients with BRAFV600E mutant colorectal cancer treated with cetuximab and encorafenib +/- binimetinib or alpelisib. *Br J Cancer* 124:176-182, 2021
17. Elez E, Ros J, Fernández J, et al: RNF43 mutations predict response to anti-BRAF/EGFR combinatory therapies in BRAFV600E metastatic colorectal cancer. *Nat Med* 28:2162-2170, 2022
18. Mundt F, Nielsen AB, Duel JK, et al: In depth profiling of the cancer proteome from the flowthrough of standard RNA-preparation kits for precision oncology. *bioRxiv* 10.1101/2023.05.12.540582
19. Yaffe MB: Why geneticists stole cancer research even though cancer is primarily a signaling disease. *Sci Signal* 12:eaaw3483, 2019
20. Mertins P, Mani DR, Ruggles KV, et al: Proteogenomics connects somatic mutations to signalling in breast cancer. *Nature* 534:55-62, 2016
21. Wang J, Ma Z, Carr SA, et al: Proteome profiling outperforms transcriptome profiling for coexpression based gene function prediction. *Mol Cell Proteomics* 16:121-134, 2017
22. Mundt F, Rajput S, Li S, et al: Mass spectrometry-based proteomics reveals potential roles of NEK9 and MAP2K4 in resistance to PI3K inhibition in triple-negative breast cancers. *Cancer Res* 78:2732-2746, 2018
23. Tuxen IV, Rohrberg KS, Oestrup O, et al: Copenhagen prospective personalized oncology (CoPPD)—Clinical utility of using molecular profiling to select patients to phase I trials. *Clin Cancer Res* 25:1239-1247, 2019
24. Eisenhauer EA, Therasse P, Bogaerts J, et al: New response evaluation criteria in solid tumours: Revised RECIST guideline (version 1.1). *Eur J Cancer* 45:228-247, 2009
25. Richards S, Aziz N, Bale S, et al: Standards and guidelines for the interpretation of sequence variants: A joint consensus recommendation of the American College of Medical Genetics and Genomics and the Association for Molecular Pathology. *Genet Med* 17:405-424, 2015
26. H: Hallmark gene sets - The Molecular Signatures Database - GSEA. <https://www.gsea-msigdb.org/gsea/msigdb/index.jsp>
27. Santos A, Colaço AR, Nielsen AB, et al: A knowledge graph to interpret clinical proteomics data. *Nat Biotechnol* 40:692-702, 2022
28. UBE2K ubiquitin conjugating enzyme E2 K [Homo sapiens (human)]—Gene—NCBI. <https://www.ncbi.nlm.nih.gov/gene/3093>
29. Aubrey BJ, Strasser A, Kelly GL: Tumor-suppressor functions of the TP53 pathway. *Cold Spring Harb Perspect Med* 6:a026062, 2016
30. Kastenhuber ER, Lowe SW: Putting p53 in context. *Cell* 170:1062-1078, 2017
31. Molecular genetics of colorectal cancer. annual review of pathology: Mechanisms of disease. <https://www-annualreviews-org.ep.fjrnadgang.kb.dk/doi/10.1146/annurev-pathol-011110-130235>
32. Schell MJ, Yang M, Teer JK, et al: A multigene mutation classification of 468 colorectal cancers reveals a prognostic role for APC. *Nat Commun* 7:11743, 2016
33. Cisowski J, Sayin VI, Liu M, et al: Oncogene-induced senescence underlies the mutual exclusive nature of oncogenic KRAS and BRAF. *Oncogene* 35:1328-1333, 2016
34. Chen ZJ, Niles EG, Pickart CM: Isolation of a cDNA encoding a mammalian multiubiquitinating enzyme (E225K) and overexpression of the functional enzyme in Escherichia coli. *J Biol Chem* 266:15698-15704, 1991
35. Kalchman MA, Graham RK, Xia G, et al: Huntingtin is ubiquitinated and interacts with a specific ubiquitin-conjugating enzyme. *J Biol Chem* 271:19385-19394, 1996
36. Lei X, Hu X, Lu Q, et al: UBE2K promotes the malignant progression of hepatocellular carcinoma by regulating c-Myc. *Biochem Biophys Res Commun* 638:210-218, 2023
37. Wang Q, Dong Z, Su J, et al: Ixazomib inhibits myeloma cell proliferation by targeting UBE2K. *Biochem Biophys Res Commun* 549:1-7, 2021
38. Hong NH, Tak YJ, Rhim H, et al: Hip2 ubiquitin-conjugating enzyme has a role in UV-induced G1/S arrest and re-entry. *Genes Genom* 41:159-166, 2019
39. Nastke M-D, Permatteo M, Sundararajan P, et al: Abstract 5321: BRG399: A novel potent small molecule modulator of UBE2K for the treatment of various cancers. *Cancer Res* 82:5321, 2022 (suppl 12)
40. Karoulia Z, Gavathiotis E, Poulikakos PI: New perspectives for targeting RAF kinase in human cancer. *Nat Rev Cancer* 17:676-691, 2017
41. Poulikakos PI, Persaud Y, Janakiraman M, et al: RAF inhibitor resistance is mediated by dimerization of aberrantly spliced BRAF(V600E). *Nature* 480:387-390, 2011
42. Yao Z, Torres NM, Tao A, et al: BRAF mutants evade ERK-dependent feedback by different mechanisms that determine their sensitivity to pharmacologic inhibition. *Cancer cell* 28:370-383, 2015
43. Karoulia Z, Wu Y, Ahmed TA, et al: An integrated model of RAF inhibitor action predicts inhibitor activity against oncogenic BRAF signaling. *Cancer Cell* 30:485-498, 2016